

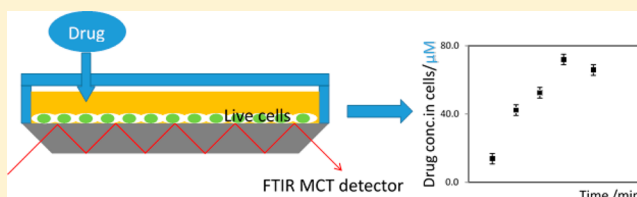
Label-Free in Situ Quantification of Drug in Living Cells at Micromolar Levels Using Infrared Spectroscopy

K. L. Andrew Chan* and Pedro L. V. Fale

Institute of Pharmaceutical Science, King's College London, London SE1 9NH, U.K.

Supporting Information

ABSTRACT: Quantifying the rate and the amount of drug entering live cells is an essential part of the medicine development process. Infrared spectroscopy is a label-free, chemically selective tool for analyzing the composition of live cells in culture that has the potential to quantify, in situ, the amount of drug entering living cells in a nondestructive manner, although its sensitivity is currently limited. This paper is the first to demonstrate in situ quantification of the cancer drug, fluorouracil, in live cells at a therapeutically relevant concentration using Fourier transform infrared spectroscopy. To achieve the required improvement in detection and quantitation limits of the IR measurement, two strategies were exploited. First, a sampling method called multibounce attenuated total reflection was used to optimize the signal while second, a long pass filter in combination with a mercury cadmium telluride detector was used to reduce the instrument noise. Using these novel adaptations, it was possible to quantify 20 μM of fluorouracil in cell culture medium using a standard FTIR instrument, while it was possible to quantify and measure the flux of fluorouracil in situ in living cells treated with an 80 μM drug.



The ability to measure drug concentration in living cells in a selective, nondestructive manner and without recourse to labeling the drug has the important advantage of eliminating any unwanted and/or unexpected interference to the drug's natural diffusive processes. The analytical method should therefore be able to detect and quantify the drug at therapeutic concentrations under biological relevant conditions. The precise concentration to be detected, however, depends upon the drug under investigation, with a recent study¹ of the cancer drug fluorouracil (5-FU) indicating that plasma concentrations 5, 19, and 31 min after a patient receiving a 370 mg/m² dose of 5-FU were 110, 60, and 15 μM , respectively.

Fourier transform infrared (FTIR) spectroscopy is a widely available analytical technique that enables a label-free and nondestructive analysis of drug molecules. One area where FTIR spectroscopy is increasingly finding application is the measurement of living cells, including single cells^{2–6} and populations of cells,^{7–9} such as the characterization of normal cells from carcinoma,² response of cells to mechanical stress,³ chemical stress,⁴ optical stimulation,⁵ protein aggregation,¹⁰ cell attachment,^{11–13} cell death,^{14,15} cell differentiation,¹⁶ and cell activation.^{17,18} One factor that limits the use of FTIR for drug analysis in living cells is the water band that dominates the IR spectra and which arises from water being the major component of living cells. Due to the low concentrations of drug that are generally present in the body, the presence of the water band in the IR spectrum limits the quantification and detection limit of the analysis of drug diffusion into cells. However, FTIR spectra of living cells when obtained with high signal-to-noise ratios (SNR) will, after the subtraction of water band, reveal the spectral features of components of interest that are of low concentrations such as the added drug in the living

cells. The intrinsic SNR of a spectrometer can be estimated by the following equation¹⁹

$$\text{SNR} = \Theta \xi U \Delta \nu D \left(\frac{t}{A_D} \right)^{1/2} \quad (1)$$

The equation implies that SNR is proportional to Θ (the throughput of light), ξ (spectrometer efficiency), U (spectral energy density), $\Delta \nu$ (spectral resolution), D (detector sensitivity), and \sqrt{t} (time or the number of coadditions) and inversely proportional to $\sqrt{A_D}$ (the detector area).¹⁹

Although it is possible to increase detector sensitivity (D) and therefore SNR by employing a highly sensitive liquid-nitrogen-cooled mercury cadmium telluride (MCT) detector instead of room temperature detectors such as lithium tantalum oxide (LiTaO₃) or deuterated triglycine sulfate (DTGS) detectors, MCT detectors are only advantageous in situations where the throughput of light is low. Highly sensitive MCT detectors are easily saturated and, consequently, attenuators or small apertures are often employed to reduce the throughput of light (Θ) to ensure that saturation of the detector does not occur, thereby reducing the advantage gained from increasing D by use of a more sensitive detector.

One way to overcome this problem is the realization that most of the useful spectral information is contained in the carbonyl to fingerprint region (namely 1800–500 cm⁻¹) and that by using a long pass filter, it is possible to reduce the

Received: August 1, 2014

Accepted: November 6, 2014

Published: November 6, 2014

overall intensity of light and hence avoid saturating the MCT detector without reducing the throughput of light in the spectral region of interest. Although long pass filters have been previously used to increase scan speed in FTIR imaging experiments,^{20,21} and the signal-to-noise of spectra in difference FTIR spectroscopy of bacteria,²² to our knowledge, they have not been used to improve the SNR of a FTIR measurement of drug in solution and in living cells. To optimize the spectral signal from the living cells and minimize the disturbance from the culturing medium, the multibounce attenuated total reflection (ATR) measurement mode where only the living cells adhered to the measuring surface of the ATR element (Figure 1) is measured. Increasing the path length in the living

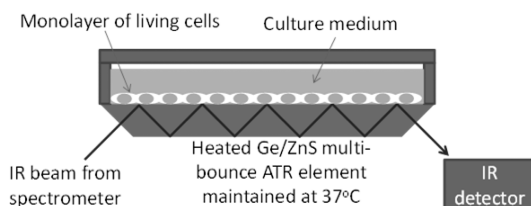


Figure 1. Schematic of a multibounce ATR FTIR measurement setup. The IR beam interacts with the sample with a depth of penetration of typically a few micrometers, which is deep enough to measure absorbance from the bulk of the adherent cells but shallow enough to avoid absorbance from the culture medium. The signal from the cell can therefore be increased by using the multibounce ATR method without unwanted attenuation of light from the culture medium. The size and thickness of the multibounce ATR element can be chosen to achieve the optimal path length. The signal from the analyte is proportional to the number of bounces (and hence the total path length) used in the ATR measurement.

cell can significantly increase the signal, hence the sensitivity and the detection limit, when compared to transmission measurement. However, increasing the path length will also increase the noise and, therefore, an optimal path length for the measurement of living cell has been investigated (details can be found in Figure S-1 of the Supporting Information).

The present work demonstrates the potential of using a long pass IR filter in combination with a zinc sulfide (ZnS) multibounce ATR, which produce the optimal path length, FTIR measurement to acquire spectra of aqueous drug solution and live cells under treatment of drug with a sufficiently improved SNR to enable quantification of drug in living cells. Aqueous solutions of the drug, 5-fluorouracil (5-FU), at therapeutically relevant concentrations of between 10–700 μM , were used as test samples to demonstrate the level of detection and quantitation limits that can be achieved using this relatively simple methodology. Many cell lines were found to adhere and grow well on the ZnS substrate as demonstrated by Wehbe et al.²³ as well as from our preliminary tests against HeLa, macrophage, PC-3, and insulin-secreting beta (INS) cell lines. In this study, the INS cell line was used as the test cells. Difference FTIR spectra of drug diffusing in living cell were also determined to demonstrate the low noise levels that can be achieved using this approach, and HPLC was used as an orthogonal method to confirm the results obtained.

EXPERIMENTAL SECTION

Multibounce ATR FTIR Accessory. A temperature controlled 20 bounce (10 bounces on the measurement side) ATR accessory trough plate (HATR, Pike technologies) and a

45° ZnS ATR element (Crystran Ltd., U.K.) was used. The trough plate has a measurement area of $\sim 500 \text{ mm}^2$, where the living cells can attach and be measured. The approximate area occupied by attached insulin-secreting beta cells (INS) is $1.7 \times 10^{-4} \text{ mm}^2$. It is therefore estimated that at 100% confluence, ~ 3 million cells can be attached and measured.

Live Cell Preparation. Insulin secreting beta cells (INS cell line, kindly provided by Dr Andrei Tarasov from University of Oxford) were maintained in T25 cell culture flasks using RPMI medium supplemented with 10% FBS and 2 mM L-glutamine, in a 5% CO_2 environment at 37 °C. The cells were trypsinised and harvested when they had reached $\sim 80\%$ confluence. The cells were then centrifuged into a pellet and resuspended in L15 medium supplemented with 10% FBS, 2 mM L-glutamine, 100 U/mL penicillin, and 100 U/mL streptomycin. L15 was used to allow closed chamber culturing with air as the gaseous phase. The cell suspension was diluted in 10 mL of medium to reach a cell density of $\sim 1.2 \times 10^6$ cell per mL and 2.5 mL of the resulting cell suspension (i.e., ~ 3 million of cells) seeded directly onto the multibounce, temperature-controlled ATR trough which was then well-sealed and maintained at 35 °C and covered with a warm blanket to prevent evaporation. After incubating overnight, the relatively high cell seeding density ensured a high confluency of cells adhered to the measuring surface. The cells were incubated for a further 2 h with the spectrum of the cell monitored at a 4 min interval. Experiments were conducted when the change in the spectrum of cells was stabilized and a steady but small increase in the absorbance of the cells was established.

Drug Solutions Preparation. A 5 and 10 mM stock solutions of fluorouracil (5-FU, Sigma-Aldrich, U.K.) in L15 media were produced by dissolving the required amount of 5-FU in the medium and stirring until dissolved. To build the calibration curves, standard solutions of 5-FU were produced by diluting the 5 mM stock solution in L15 media to obtain 10, 20, 30, 40, 50, 100, and 190 μM for the system with the MCT detector and 200, 300, 400, 600, 800, 1000, and 1200 μM for the system with the LiTaO₃ detector.

FTIR Measurement of Samples. Continuous scan FTIR spectrometers (Frontier, PerkinElmer) were fitted with a LiTaO₃, a DTGS, and a MCT detector and a long pass filter (IR LWP filter at 5.5 μm , Infrared Filter Solution Ltd.) to allow selection of the IR bands with wavenumber below 1850 cm^{-1} passing to the sample chamber. The cells on the ATR element were exposed to 80 or 400 μM of drug by adding 20 or 105 μL of the 10 mM stock solution of 5-FU to the cell culture on the trough plate, which has a volume of medium of 2.5 mL. The cells exposed to 80 μM of 5-FU were measured using the MCT detector with the long pass filter, while the cells exposed to 400 μM of 5-FU were measured using the LiTaO₃ detector, both with a scanning time of 4 min. The standard solutions for the calibration curves were measured using the MCT detector with the long pass filter, the DTGS detector, and the LiTaO₃ detector with a scanning time of 4 min. Deionized water was measured using the LiTaO₃ and the DTGS detector without attenuation of light, the MCT detector with attenuation of light by the means of a small aperture, and the MCT detector with attenuation of light by the means of the long pass filter and with a scanning time of 1 min. All measurements were acquired with a spectral resolution of 8 cm^{-1} and a spectral range of 4000–900 cm^{-1} or 1850–900 cm^{-1} (when the long pass filter is used). The strong Norton-Beer apodization function and self-phase correction was chosen for the process of the interfero-

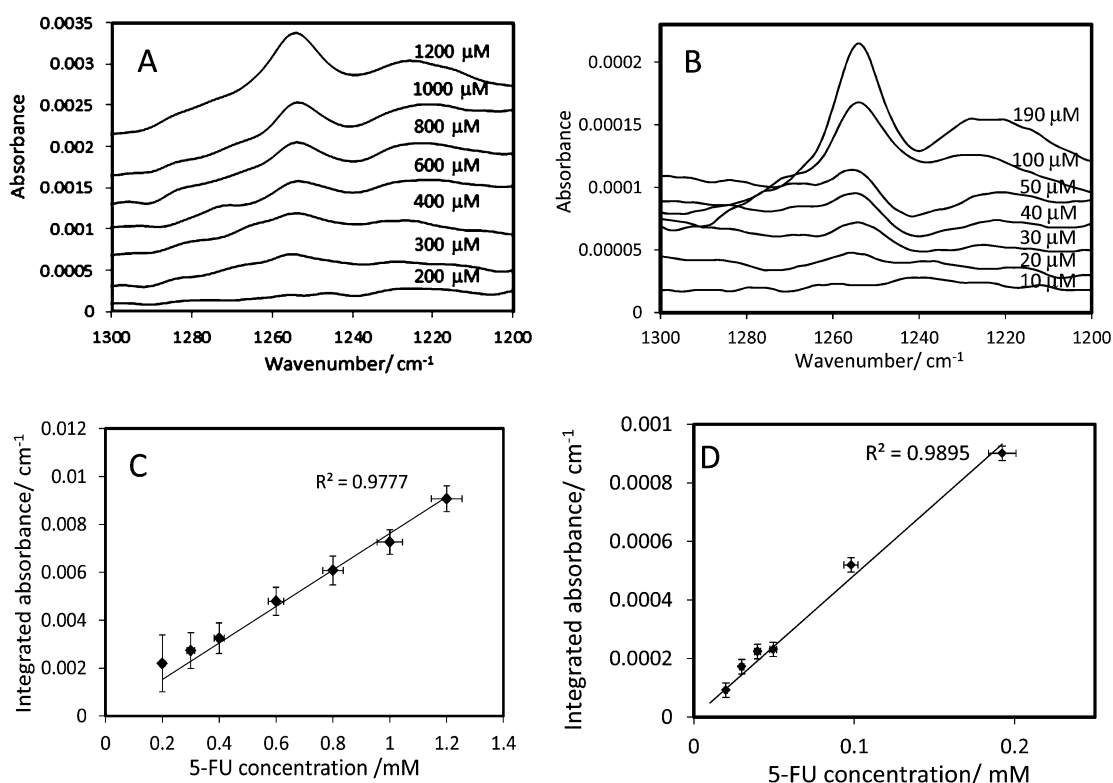


Figure 2. Difference IR spectra of 5-FU in medium at various concentration levels measured with (A) a LiTaO₃ detector and (B) a MCT detector with a long pass filter. (C and D) Calibration curves obtained from the measurement of a set of standard samples of known 5-FU drug concentrations. (C) Measurement with a LiTaO₃ detector. (D) Measurement with a MCT detector with a long pass filter. The integrated absorbance is calculated based on the band at 1254 cm⁻¹ with a straight baseline between the points, 1264 and 1243 cm⁻¹. The vertical error bars represent the contribution from spectral noise, and the horizontal error bars represent the uncertainties arising from the dilution of the drug solution.

gram. Spectrum 10 (PerkinElmer) was used for all data processing.

HPLC Measurement of Intracellular 5-FU Concentration. INS cells were seeded in 12 well plates, in similar conditions to the ones used for the ATR-FTIR experiments, using the same medium and cell density (~1 million cells/well). The cells were incubated at 37 °C until settling and reaching confluence. 5-FU was added at a concentration of 80 μM. At times 0, 4, 8, 16, and 24 min after the addition of 5-FU, the cells were washed three times with PBS, resuspended in 500 μL of 50% MeOH/H₂O, sonicated 5 × 10 s, centrifuged 10 min at 5000g, and the supernatant was analyzed by HPLC.

The HPLC–UV/vis analysis of 5-FU was carried out in a Jasco 2000Plus HPLC system equipped with a Column Oven CO-2067Plus and UV/vis Detector UV-2075Plus. A column Phenomenex Gemini-NX 5 μm C18 110A was used. Twenty five microliters of sample was injected, and an elution gradient consisting of methanol and water²⁴ was used as following: 0 min, 2% methanol; 8 min, 10% methanol; 15 min, 80% methanol; 17 min, 80% methanol, with a flow of 1.000 mL/min. The detection was carried out at 260 nm. A 5-FU calibration curve built by injecting standard solutions at the concentrations of 0, 0.5, 2, 10, 20, and 100 μM in the same conditions. The intracellular volume was calculated after determination of the cell pellet volume, after centrifugation for 10 min at 600g, in triplicate from the same batch of cells.²⁵

RESULTS AND DISCUSSION

Deionized water was first used as test solution to demonstrate the reduced noise level achievable with the long pass filter. The

result (see Figure S-2 of the Supporting Information) shows that the measurement using the DTGS detector and the MCT detector without the long pass filter exhibited similar peak-to-peak noise levels of ~0.018% or a SNR of ~5500 while the LiTaO₃ has a higher noise level of ~0.05% or a SNR of ~2000. The reason why the SNR was not significantly improved when using the MCT detector despite the sensitivity, *D*, is an order of magnitude higher than the DTGS or the LiTaO₃ detector is because the light source was attenuated by means of an aperture to avoid the saturation of the MCT detector. However, when the light was attenuated by a long pass filter that cut off IR light with wavenumber above 1850 cm⁻¹ instead of a small aperture, it is clear that the measurement can be performed without the attenuation of light in the 1500–1000 cm⁻¹ region. Significantly, the noise level is greatly improved with the peak-to-peak noise level in the 1500–1000 cm⁻¹ region of ~0.003% or a SNR of 33000 (see Figure S-2 of the Supporting Information), which is a 6-fold improvement compared to the DTGS detector and more than 15-fold improvement compared to the LiTaO₃ detector without an increase in scan time or reduction of spectral resolution.

The limits of detection in cell culture medium using the LiTaO₃, the DTGS, and the MCT detector coupled with the long pass filter have been compared using 5-FU as the test drug. 5-FU was selected because it is a widely used, and therefore relevant, drug molecule. Furthermore, the drug is studied at an in vitro concentration of 10 μM–1 mM,²⁶ which should be detectable using the methodology in the present study. 5-FU has a number of major spectral bands in the IR ν(C=O) and fingerprint region, including a relatively broad band at 1690

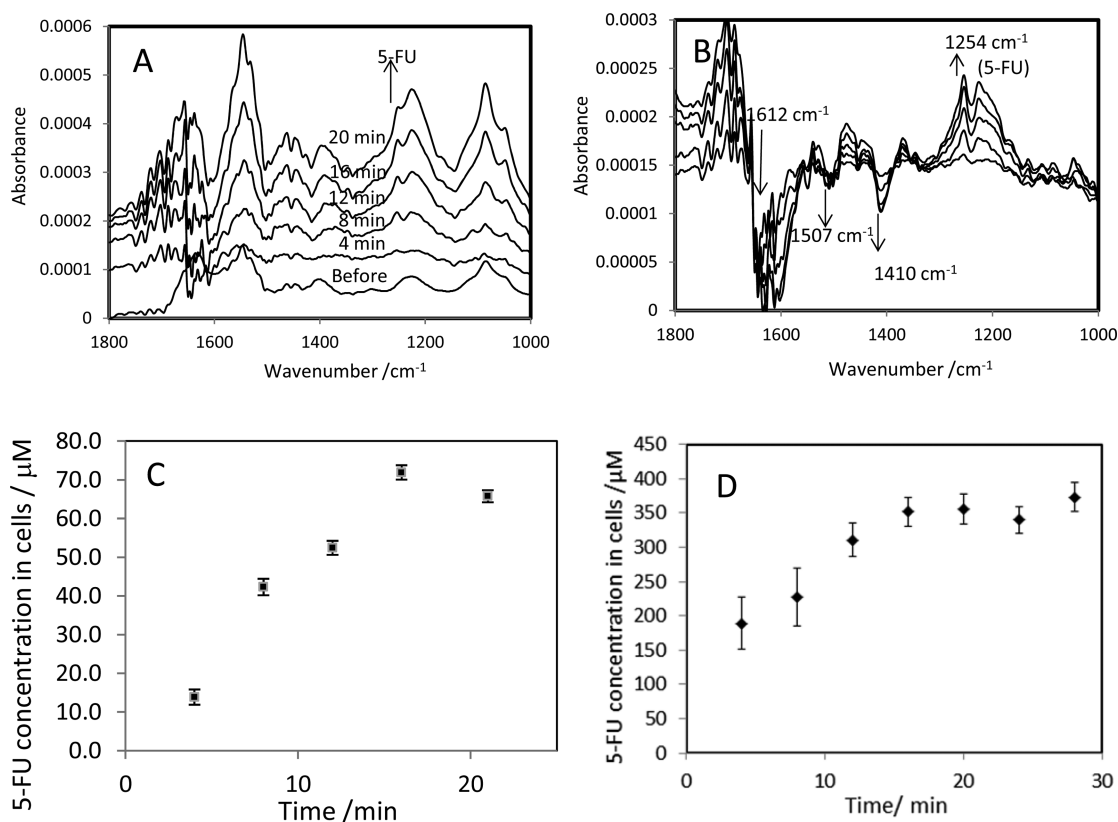


Figure 3. (A) Difference FTIR spectra of the living cell measured using the MCT detector with the low-pass filter before and after the addition of 80 μM of drug in the medium. The “before” spectrum is the difference between two consecutive FTIR measurements of the cells with 4 min time intervals before the addition of drug. The “4 min”, “8 min”, ..., “20 min” spectra are the difference between the spectrum of the living cell measured immediately after the addition of the drug and the spectrum measured at 4, 8, ..., 20 min after the addition of the drug. (B) Difference spectra of the living cells after the addition of drug with the contribution from the growth of the living cells subtracted to highlight the changes in the living cell composition as a result of the added drug. (C) A plot showing the concentration of 5-FU measured in the living cell as a function of time after the addition of 80 μM of the drug in the medium using the MCT detector with the low-pass filter. (D) A repeat experiment of (C) measured with the LiTaO_3 detector and an increased concentration of 5-FU of 400 μM . Error bars representing the uncertainties from the spectral noise.

cm^{-1} and a sharp band at 1254 cm^{-1} (see Figure S-3 of the Supporting Information). The band at 1690 cm^{-1} is slightly stronger than the 1254 cm^{-1} band, but it overlaps with the stronger water band at 1640 cm^{-1} and therefore is not a suitable marker for the current analysis. The band at 1254 cm^{-1} is in a region where water has relatively low absorbance and therefore absorbance of this band was used to construct the calibration curve. The difference IR spectra of drug in medium showing the 5-FU band at 1254 cm^{-1} as determined using the LiTaO_3 and MCT detectors are shown in Figure 2 (panels A and B). Results from the DTGS detector are shown in Figure S-4 of the Supporting Information. Figure 2A shows that the drug is detectable at a concentration of 300 μM and above when the LiTaO_3 detector is used in a 4 min measurement. However, when the MCT detector is used in combination with the long pass filter, 5-FU is detectable at 20 μM (Figure 2B). Calibration curves extracted from these data are shown in Figure 2 (panels C and D). When using the LiTaO_3 detector, the peak-to-peak noise of the absorbance spectra (Figure 2A) is $\sim 75\text{ }\mu\text{a.u.}$ (estimated by measuring the absorbance difference between the peak and trough in the $1300\text{--}1270\text{ cm}^{-1}$ region), while the peak height of the 5-FU band at 300 μM is $\sim 230\text{ }\mu\text{a.u.}$ (estimated by measuring the difference in absorbance between the peak at 1254 cm^{-1} to the baseline of the peak, which is a straight line from 1280 to 1200 cm^{-1}) giving a SNR of 3, which is considered as just detected. In contrast, when the MCT

detector is used in combination with the long pass filter, the peak-to-peak noise, estimated in the same way as the data measured with LiTaO_3 detector (Figure 2B), is $\sim 2\text{ }\mu\text{a.u.}$ while the peak height of the drug band at 20 μM is $\sim 15\text{ }\mu\text{a.u.}$, which gives a SNR of 7.5. Furthermore, when measured with the MCT detector combined with the long pass filter, the calibration curve for 5-FU is linear down to 20 μM 5-FU. Therefore, using the LiTaO_3 detector limits the study of 5-FU in the cell culture to, at best, 300 μM , while the MCT detector with the long pass filter gives better SNR spectra and a more than 15 times better limit of detection leading to a greater accuracy at a low concentration level than is currently achieved in the in vitro studies. Using the DTGS detector, the detection limit is found to be 170 μM (Figure S-4 of the Supporting Information), which is a slight improvement when compared to the LiTaO_3 detector but is still significantly worse than the MCT detector with a long pass filter approach.

In order to demonstrate that it is possible to study the 5-FU in living cells, INS cells were used. The INS cells were used because previously it has been shown that they are able to reach near confluency on a ZnS substrate when grown in L15 culture medium, and the cell viability with this cell culturing condition has been verified with the Trypan blue assay and visible monitoring of the cell morphology (see Figure S-5 of the Supporting Information). For the in situ multibounce ATR FTIR measurements, the INS cells were seeded at relatively

high density and incubated to allow them to reach high confluency on the measuring surface of the ZnS ATR element (Figure 1). Before the addition of drug, the spectra of the living cells were monitored at a 4 min interval, and the viability and confluency of the cells was verified by monitoring the cell morphology. The difference between two consecutive measurements made at 4 min intervals shows a small increase in absorbance of the living cells (Figure 3A, spectrum “before”), indicating that there was a small increase in the amount of cells on the ATR element, which was expected from a living cell culture. The 5-FU solution was then added to the culture medium such that the concentration of 5-FU was $\sim 80 \mu\text{M}$. The first measurement acquired immediately after adding the drug was used as the reference spectrum to subtract from all the subsequent measurements, which were also acquired at 4 min intervals. Hence, the difference spectrum labeled 4 min in Figure 3A is the measurement started at 4 min after the addition of drug subtracted by the first measurement (the reference) acquired immediately after the addition of drug, and the difference spectrum labeled 8 min in Figure 3A is the measurement started at 8 min subtracted by the first measurement (the reference) after the addition of drug. Difference FTIR spectra of the cells, before and after the addition of 5-FU, are shown in Figure 3A. Since the measured signal is from the average of ~ 3 million cells (the number of cells being measured in a single measurement is estimated to be 3 million, see method for details), the cell-to-cell variations are averaged and only the total growth of the cells and the effect of the added drug are observed. Most importantly, the 5-FU band at 1254 cm^{-1} in the cells can be clearly seen and it was increasing as a function of time, indicative that the drug was diffusing into the living cells. A number of other bands that do not belong to the drug have also increased as a function of time, including the amide II band at 1540 cm^{-1} , the amide III at $\sim 1240 \text{ cm}^{-1}$, and the DNA bands at around 1080 cm^{-1} . These bands belong to the living cells as shown by the spectrum before the addition of the drug. To reduce the contribution to the spectral band, changes due to the growth of the living cells, a second subtraction of the living cell spectrum has been performed. The spectrum of the cells before the addition of the drug (the “before” spectrum in Figure 3A), which represent the spectrum of the cells without the drug, was subtracted from the spectra, also in Figure 3A, of the live cells 4, 8, 12, 16, and 20 min after the addition of the drug, and the results are shown in Figure 3B. Noting that 5-FU does not have strong absorbance in the 1080 cm^{-1} region, the DNA band of the cell at 1080 cm^{-1} was used as the indicator of complete subtraction; the subtraction is completed when the 1080 cm^{-1} band is minimized. After the subtraction, the increase in the 5-FU band at 1254 cm^{-1} is more pronounced and therefore more easily quantified. There are also other subtle changes in the spectrum of the living cells that have been detected, such as the reduction of the bands at 1612 , 1507 , and 1410 cm^{-1} . A blank medium of $20 \mu\text{L}$ without drug was added to the live cells to characterize any placebo effect. The result has shown that the addition of the blank medium did not produce the observed changes when the drug was added. These spectral changes could be a result of a change in the concentration of metabolites in the cells induced by the drug. Nevertheless, the presence of these bands does not alter the conclusions of the present study. Even though their investigation is outside the scope of this paper, it is important to highlight that the spectral changes of the living cells as a result of the addition of drug are

small (in the range of 0.0001 au), despite the relatively long path length of $\sim 30 \mu\text{m}$ used in these measurements, which further underlined the importance of achieving low noise levels in the study of living cells using FTIR spectroscopy. The amount of 5-FU in the living cells has been quantified by integrating the area under the band at 1254 cm^{-1} of the spectra shown in Figure 3B and using the calibration curve shown in Figure 2D, and the result is shown in Figure 3C. The concentration of drug increases as a function of time and reached equilibrium after $\sim 16 \text{ min}$ at a drug concentration of $\sim 70 \mu\text{M}$, which is slightly below the concentration of drug in the medium. The experiment was repeated using the LiTaO_3 detector, and it was found that the drug concentration applied was required to be increased to $400 \mu\text{M}$ before the 5-FU can be detected in the living cells (see Figure 3D). Nevertheless, using the calibration curve in Figure 2C, the diffusion profile is obtained, which is remarkably similar to Figure 3C showing a steady increase of the concentration of drug in the cells and reaching a plateau at 16 min. Figure 3C also shows that the concentration of drug in the cells increases linearly with time and a flux of drug of $0.4 \text{ nmol m}^{-2} \text{ s}^{-1}$ can be calculated from the gradient. However, the experiment will benefit from higher temporal resolution, which can be achievable with slightly lowered SNR.

The drug concentrations in cells were also measured using the standard HPLC method (Figure 4), based on a method

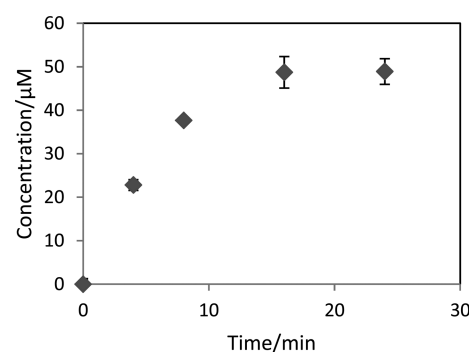


Figure 4. Ex situ quantification of intracellular concentration of 5-FU by HPLC 0, 4, 8, 16, and 24 min after addition of the drug. Error bars represent standard deviation from triplicates.

previously described for the quantification of 5-FU.²⁴ The HPLC method showed linearity in a concentration range appropriate for the intracellular concentration of 5-FU, between 0.5 and $100 \mu\text{M}$, and a calibration curve with R^2 of 0.9997 was built with the area of the 5-FU peak detected at 260 nm . The intracellular drug concentration measured by HPLC reached an equilibrium at the same time as in the FTIR experiments, after approximately 16 min, but at a value of 50 instead of $70 \mu\text{M}$. This difference may be due to the method used in the measurement of cell volume in the HPLC experiment, which may include gaps between cells, extracellular matrix, and the cellular membrane itself, leading to a slight overestimation of the overall volume of the cells, hence a slight underestimation of the concentration of drug. The FTIR data, on the other hand, are directly collected from the cytoplasm, therefore providing a more accurate measure of the intracellular concentration. Comparing to a previous ex situ measurement of radio-labeled 5-FU concentration in Lettre cells, the diffusion of drug to the INS cells appears to be slower and does not show the partitioning effect.²⁶ As pointed out in that work, however,

the ratio of internal and external cellular drug concentration is a function of the pH gradient which was not determined in the current study. Furthermore, a different cell line was used in that previous study which can lead to the different response observed. A direct comparison of the drug diffusion in different cell lines will be a future study.

CONCLUSION

Significantly, this work has demonstrated that highly sensitive measurement of drug concentration in living cells can be achieved with equipment that is readily available in many laboratories or, at most, requires the purchase of a small multibounce ATR accessory. The cost of the filter and the multibounce ATR accessory that is needed to perform this experiment is minimal compared to other more sophisticated label-free techniques that may be used for the measurement of drug concentration in living cells such as stimulated Raman scattering.²⁷ The method developed here is both relatively straightforward, with minimal interference by extrinsic factors and nondestructive, allowing the living cells to undergo further analysis if necessary. Measurement of drug concentration in living cells has been demonstrated using INS cells, but other cell lines such as HeLa and PC-3 have also been successfully tested for other ongoing studies, whose results will be reported in separate publications. The increase in drug concentration as a function of time has been quantified using the multibounce ATR FTIR system demonstrating that this method is suitable to track the process of drug diffusion in living cells in a label-free and nondestructive manner.

It is important to note that the SNR can be further improved by using a nitrogen purge or else by fully upgrading the spectrometer (e.g., to a vacuum system with gold coated mirrors) to increase the throughput of light and eliminate the atmospheric contribution to the noises in the background. New developments in infrared spectroscopy such as the use of quantum cascade laser as the infrared source²⁸ may further improve the sensitivity of this technique to allow the detection of drug in nanomolar levels. Nevertheless, this work has demonstrated that the sensitivity provided with the presented technique is high enough to measure the 5-FU drug in living cells at a clinical relevant concentration level, using standard FTIR equipment.

In summary, the method has been demonstrated to be a viable tool for detecting and quantifying drugs and other relevant biomolecules in living cells without the need for additional labeling. This method can be applied for studying drug efficacy, drug screening purposes in the development of new drugs, or as a tool to understand the mechanism of drug resistance.

ASSOCIATED CONTENT

Supporting Information

Optical path length for FTIR measurements of live cells; a summary of the number of bounces required; a plot showing the relationships between the relative SNR and path length at different spectral regions when the analyte is measured in water; ratio of the intensity of two consecutive measurements with deionized water on the ZnS ATR element; spectrum of pure 5-FU solution in the 1800–1000 cm⁻¹ region; difference IR spectra of 5-FU in medium at various concentration levels and calibration curve obtained from the measurement; and visible image of live cells on ZnS substrate in L15 medium. This

material is available free of charge via the Internet at <http://pubs.acs.org>.

AUTHOR INFORMATION

Corresponding Author

*E-mail: ka_lung.chan@kcl.ac.uk.

Notes

The authors declare no competing financial interest.

ACKNOWLEDGMENTS

The project is supported by the Royal Society and EPSRC (EP/L013045/1). We thank Professor Jayne Lawrence for her advice and discussion on this work, Dr Tarasov for discussion and for providing the INS cell line used in this study, Prof. Sergei Kazarian for providing the 5-FU drug and Miss Hoi Yan Chan for early stage cell culture work.

REFERENCES

- (1) Kosovec, J. E.; Egorin, M. J.; Gjurich, S.; Beumer, J. H. *Rapid Commun. Mass Spectrom.* **2008**, *22*, 224–230 DOI: 10.1002/rcm.3362.
- (2) Zhao, R.; Quaroni, L.; Casson, A. G. *Analyst* **2010**, *135*, 53–61 DOI: 10.1039/b914311d.
- (3) Birarda, G.; Greci, G.; Businaro, L.; Marmioli, B.; Pacor, S.; Piccirilli, F.; Vaccari, L. *Vib. Spectrosc.* **2010**, *53*, 6–11 DOI: 10.1016/j.vibspec.2010.01.016.
- (4) Munro, K. L.; Bamberg, K. R.; Carter, E. A.; Puskar, L.; Tobin, M. J.; Wood, B. R.; Dillon, C. T. *Vib. Spectrosc.* **2010**, *53*, 39–44 DOI: 10.1016/j.vibspec.2010.02.004.
- (5) Quaroni, L.; Zlateva, T.; Normand, E. *Anal. Chem.* **2011**, *83*, 7371–7380 DOI: 10.1021/ac201318z.
- (6) Kuimova, M. K.; Chan, K. L. A.; Kazarian, S. G. *Appl. Spectrosc.* **2009**, *63*, 164–171.
- (7) Marcsisin, E. J.; Uttero, C. M.; Miljkovic, M.; Diem, M. *Analyst* **2010**, *135*, 3227–3232 DOI: 10.1039/c0an00548g.
- (8) Marcsisin, E. J.; Uttero, C. M.; Mazur, A. I.; Miljkovic, M.; Bird, B.; Diem, M. *Analyst* **2012**, *137*, 2958–2964 DOI: 10.1039/c2an15868j.
- (9) Hutson, T. B.; Mitchell, M. L.; Keller, J. T.; Long, D. J.; Chang, M. J. W. *Anal. Biochem.* **1988**, *174*, 415–422 DOI: 10.1016/0003-2697(88)90040-1.
- (10) Miller, L. M.; Bourassa, M. W.; Smith, R. J. *Biochim. Biophys. Acta, Biomembr.* **2013**, *1828*, 2339–2346 DOI: 10.1016/j.bbamem.2013.01.014.
- (11) Schmidt, M.; Wolfram, T.; Rumpler, M.; Tripp, C. P.; Grunze, M. *Biointerphases* **2007**, *2*, 1–5 DOI: 10.1116/1.2710336.
- (12) Miyamoto, K. I.; Yamada, P.; Yamaguchi, R. T.; Muto, T.; Hirano, A.; Kimura, Y.; Niwano, M.; Isoda, H. *Cytotechnology* **2007**, *55*, 143–149 DOI: 10.1007/s10616-007-9111-2.
- (13) Yang, W. Y.; Xiao, X. L.; Tan, J.; Cai, Q. Y. *Vib. Spectrosc.* **2009**, *49*, 64–67 DOI: 10.1016/j.vibspec.2008.04.016.
- (14) Yamaguchi, R.-t.; Hirano-Iwata, A.; Kimura, Y.; Niwano, M.; Miyamoto, K.-i.; Isoda, H.; Miyazaki, H. *Appl. Phys. Lett.* **2007**, *91*, 203902 DOI: 10.1063/1.2813013.
- (15) Yamaguchi, R.-t.; Hirano-Iwata, A.; Kimura, Y.; Niwano, M.; Miyamoto, K.-i.; Isoda, H.; Miyazaki, H. *J. Appl. Phys.* **2009**, *105*, 024701 DOI: 10.1063/1.3068203.
- (16) Aonuma, Y.; Kondo, Y.; Hirano-Iwata, A.; Nishikawa, A.; Shinohara, Y.; Iwata, H.; Kimura, Y.; Niwano, M. *Sens. Actuators, B* **2013**, *176*, 1176–1182 DOI: 10.1016/j.snb.2012.10.030.
- (17) Alam, M. K.; Timlin, J. A.; Martin, L. E.; Williams, D.; Lyons, C. R.; Garrison, K.; Hjelle, B. *Vib. Spectrosc.* **2004**, *34*, 3–11 DOI: 10.1016/j.vibspec.2003.07.002.
- (18) Timlin, J. A.; Martin, L. E.; Lyons, C. R.; Hjelle, B.; Alam, M. K. *Vib. Spectrosc.* **2009**, *50*, 78–85 DOI: 10.1016/j.vibspec.2008.07.017.
- (19) Griffiths, P. R.; De Haseth, J. A. *Fourier Transform Infrared Spectrometry*; Wiley: New York, 1986.

- (20) Chan, K. L. A.; Kazarian, S. G. *Anal. Chem.* **2012**, *84*, 4052–4056 DOI: 10.1021/ac300019m.
- (21) Chan, K. L. A.; Niu, X.; deMello, A. J.; Kazarian, S. G. *Anal. Chem.* **2011**, *83*, 3606–3609 DOI: 10.1021/ac200497a.
- (22) Li, Y.; Kimura, Y.; Arikawa, T.; Wang-Otomo, Z. Y.; Ohno, T. *Biochemistry* **2013**, *52*, 9001–9008 DOI: 10.1021/bi401033y.
- (23) Wehbe, K.; Filik, J.; Frogley, M. D.; Cinque, G. *Anal. Bioanal. Chem.* **2013**, *405*, 1311–1324 DOI: 10.1007/s00216-012-6521-6.
- (24) van Kuilenburg, A. B.; van Lenthe, H.; Maring, J. G.; van Gennip, A. H. *Nucleosides, Nucleotides Nucleic Acids* **2006**, *25*, 1257–1260 DOI: 10.1080/15257770600894741.
- (25) Armbruster, C.; Vorbach, H.; Steindl, F.; El Menyawi, I. J. *Antimicrob. Chemother.* **2001**, *47*, 487–490.
- (26) Ojugo, A. S. E.; McSheehy, P. M. J.; Stubbs, M.; Alder, G.; Bashford, C. L.; Maxwell, R. J.; Leach, M. O.; Judson, I. R.; Griffiths, J. R. *Br. J. Cancer* **1998**, *77*, 873–879 DOI: 10.1038/bjc.1998.144.
- (27) Freudiger, C. W.; Min, W.; Saar, B. G.; Lu, S.; Holtom, G. R.; He, C. W.; Tsai, J. C.; Kang, J. X.; Xie, X. S. *Science* **2008**, *322*, 1857–1861 DOI: 10.1126/science.1165758.
- (28) Mukherjee, A.; Bylund, Q.; Prasanna, M.; Margalit, Y.; Tihan, T. *J. Biomed. Opt.* **2013**, *18*, 036011 DOI: 10.1117/1.jbo.18.3.036011.